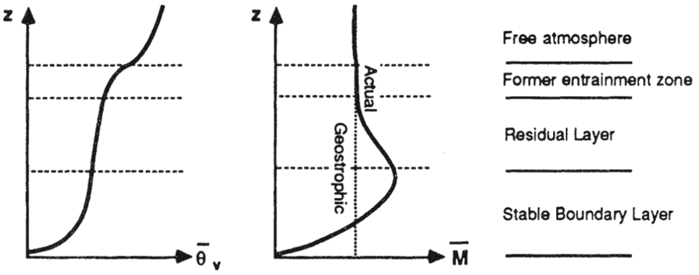

Fig. 1.11 Mean virtual potential temperature, $\overline{\theta}_v$, and wind speed, $\overline{M}$, profiles for an idealized stable boundary layer in a high-pressure region.

that, the wind speed is smaller and closer to its geostrophic value. The strong shears below the jet are accompanied by a rapid change in wind direction, where the lower level winds are directed across the isobars towards low pressure.

Touching the ground, however, is a thin (order of a few meters) layer of ***katabatic*** or ***drainage*** winds. These winds are caused by the colder air, adjacent to the ground, flowing downhill under the influence of gravity. Wind speeds of 1 m/s at a height of 1 m are possible. This cold air collects in the valleys and depressions and stagnates there. Unfortunately, many weather stations are located in or near valleys, where the observed surface winds bear little relationship to the synoptic-scale forcings at night.

Wave motions are a frequent occurrence in the SBL. The strongly stable NBL not only supports gravity waves, but it can trap many of the higher-frequency waves near the ground. Vertical wave displacements of 100 m have been observed, although the associated wind and temperature oscillations are relatively small and difficult to observe without sensitive instruments.

SBLs can also form during the day, as long as the underlying surface is colder than the air. These situations often occur during warm-air advection over a colder surface, such as after a warm frontal passage or near shorelines.

1.6.4 Virtual Potential Temperature Evolution

Given the virtual potential temperature profiles from the previous subsections, it is useful to integrate these profiles into our concept of how the boundary layer evolves. If rawinsonde soundings were made at the times indicated by flags S1 through S6 in Fig 1.7, then Fig 1.12 shows the resulting virtual potential temperature profile evolution.

We see from these soundings that knowledge of the virtual potential temperature profile is usually sufficient to identify the parts of the boundary layer. The structure of the BL is clearly evident.

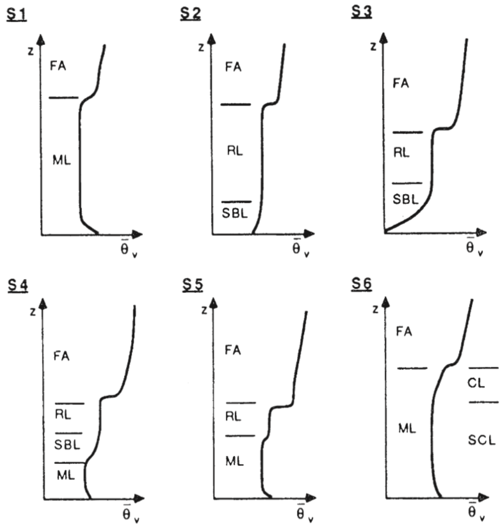

Fig. 1.12 Profiles of mean virtual potential temperature, $\bar{\theta}_v$, showing the boundary-layer evolution during a diurnal cycle starting at about 1600 local time. S1-S6 identify each sounding with an associated launch time indicated in Fig. 1.7.

Stated another way, knowledge of the virtual potential temperature lapse rate is usually sufficient for determining the static stability. An exception to this rule is evident by comparing the lapse rate in the middle of the RL with that in the middle of the ML. Both are adiabatic; yet, the ML corresponds to statically unstable air while the RL contains statically neutral air.

One way around this apparent paradox for the classification of adiabatic layers is to note the lapse rate of the air immediately below the adiabatic layer. If the lower air is superadiabatic, then both that superadiabatic layer and the overlying adiabatic layer are statically unstable. Otherwise, the adiabatic layer is statically neutral. A more precise definition of static stability is presented later.

It is obvious that as the virtual potential temperature profile evolves with time, so must the behavior of smoke plumes. For example, smoke emitted into the top of the NBL or into the RL rarely is dispersed down to the ground during the night because of the limited turbulence. These smoke plumes can be advected hundreds of kilometers downwind from their sources during the night.

Smoke plumes in the RL may disperse to the point where the bottom of the plume hits the top of the NBL. The strong static stability and frequent reduction in turbulence reduces the downward mixing into the NBL. The top of the smoke plume sometimes can continue to rise into the neutral air. This is called *lofting* (see Fig 1.13).